A study on the partial coating of a shell with an add-on viscoelastic layer for optimal damping design

Ravish S. Masti [1], **M.G. Sainsbury** [2]
[1] K.U. Leuven, Department of Mechanical Engineering, PMA
Celestijnenlaan 300B, B-3001 Heverlee
Leuven, Belgium

[2] Department of Mechanical Engineering
University of Hong Kong
Pokfulam Road, Hong Kong SAR, PR China

E-mail: ravishmasti@yahoo.co.uk

Abstract

Cylindrical shells are used in a variety of applications. In some of these applications it is necessary to limit the vibrations of lightly-damped shells by applying a damping treatment that does not significantly increase the weight. This paper explores the use of partial coating of a cylindrical shell with a constrained viscoelastic layer for obtaining optimal damping. The placement of damping patches is based on the modal strain energy intensity distribution of the undamped structure. The analysis utilizes the finite element method. Numerical studies show that a partial coating procedure can be a feasible approach for achieving an optimal damping design.

1. Introduction

Constrained viscoelastic layered treatment consists of a viscoelastic damping layer with a stiffer constraining layer on top of it. It is a popular ingredient of modern engineering design in many vibration damping applications.

Shells are often used as efficient load bearing structural members, and damping is essential when they are subjected to prohibitively large vibrations. In studies on shells *completely* covered with viscoelastic treatment, many researchers e.g., Markuš [1], Alam and Asnani [2], Ramesh and Ganesan [3], have investigated the dynamic behaviour of the damped configuration.

In critical applications requiring optimised damping design, often the constraints are limited weight and restricted space for the damping treatment. In studies on plates, for example, Ro and Baz [4] and Spalding and Mann [5] presented studies related to optimal damping.

This paper presents studies on the damping of a straight cylindrical shell partially coated with passive constrained viscoelastic patches. It investigates the effectiveness of partial coating as a treatment option in damping applications.

2. Finite elements used in the study

In the present work, the undamped shell structure is modelled using a mesh of four-node, rectangular curved shell elements of the type derived by Bogner, Fox and Schmit [6]. However, a composite curved shell element is newly derived to model the add-on constrained damping layer. This element is formulated to be compatible with the element of Bogner et al. For the sake of convenience, we refer to the element of Bogner et al. as *FEM_S* and the other as *FEM_V*. The element *FEM_V* represents a layer of viscoelastic material with a constraining layer. A discrete portion of the add-on damping treatment applied over a base shell is represented by laying *FEM_V* over *FEM_S* (see Figure 1). This is convenient in modelling a partial covering of the shell surface with the damping treatment.

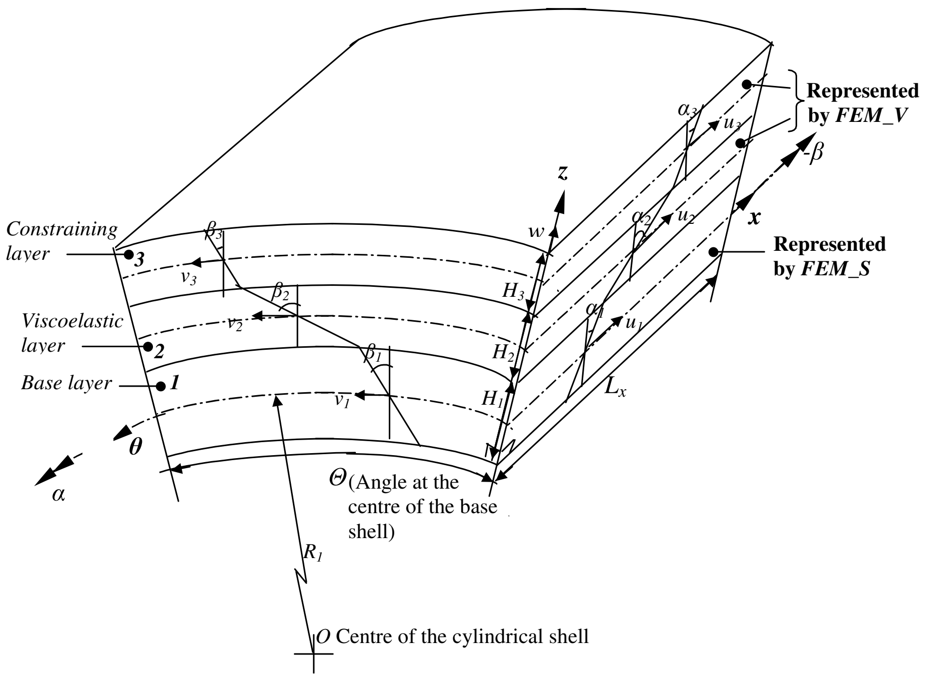

Layer 1	Represented by the element *FEM_S*
Layer 2 + Layer 3	Represented by the element *FEM_V*
x, θ and z	Coordinate directions at the reference layer - the mid-surface plane of the base shell
$u_{(1,2,3)}$,$v_{(1,2,3)}$,w	Mid-surface displacements in the respective layers. The layer numbers are identified by the subscripts
$\alpha_{(1,2,3)}$	Total rotation in the transverse plane x-z
$\beta_{(1,2,3)}$	Total rotation in the transverse plane θ-z
$H_{(1,2,3)}$	The thicknesses of the respective layers
R_1	Radius of curvature at the mid-surface plane in the base shell layer
L_x and Θ	Dimensions in x and θ directions, of the discrete damped shell

Figure 1: A discrete portion of a shell with an add-on damping treatment- represented by an element-combination *FEM_S* +*FEM_V*

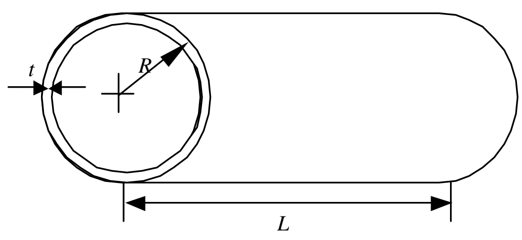

Figure 2: A complete cylindrical shell

2.1. Add-on damping layer element

The element *FEM_V* is a two-dimensional rectangular curved shell element with four corner nodes and four mid-side nodes. It is displacement-based and built using an energy formulation. The displacement variables are w, v_1, u_1, $\gamma_{\theta z_2}$ and γ_{xz_2}. Variables w, v_1, u_1 are the displacements of the mid-surface layer of the base shell, in the z (radial), θ (circumferential) and x (axial) directions respectively. Variables $\gamma_{\theta z_2}$ and γ_{xz_2} are the rotations due to shear of the viscoelastic layer, in the transverse planes θ-z *and* x-z respectively. A cubic polynomial expression is used for describing separately each of the variables w, v_1 and u_1. But, for each of the variables $\gamma_{\theta z_2}$ and γ_{xz_2}, a quadratic polynomial expression is used instead.

The nodal coordinates associated with the variables w, v_1 and u_1 are retained only at the four corner nodes of element *FEM_V*. These correspond with the nodal coordinates belonging to *FEM_S*. The nodal coordinates associated with the variables $\gamma_{\theta z_2}$ and γ_{xz_2} are retained at each of the four corner-nodes and four mid-side nodes.

Therefore, at each of the four corner-nodes of the element the nodal coordinates are w, $\frac{\partial w}{\partial x}$, $\frac{\partial w}{\partial \theta}$, $\frac{\partial^2 w}{\partial x \partial \theta}$, v_1, $\frac{\partial v_1}{\partial x}$, $\frac{\partial v_1}{\partial \theta}$, $\frac{\partial^2 v_1}{\partial x \partial \theta}$, u_1, $\frac{\partial u_1}{\partial x}$, $\frac{\partial u_1}{\partial \theta}$, $\frac{\partial^2 u_1}{\partial x \partial \theta}$, $\gamma_{\theta z_2}$ and γ_{xz_2}. And, at each of the mid-side nodes they are $\gamma_{\theta z_2}$ and γ_{xz_2}. The element *FEM_V* has a total of 64 degrees-of-freedom.

The strain-displacement relationships are obtained from Kraus [7], Sivadas and Ganesan [8]. During the course of the formulation of the element, energy integrals take into account the strain energy and kinetic energy contributions from each of the layers of the two-layer damping treatment. The strain energy and kinetic energy integrals respectively are used in building the stiffness and inertia matrices of the element. The matrix form of the equations of motion is derived using Lagrange's equation.

3. Validation test

In the main damping analysis studies on partial coating, the element *FEM_V* will be used in conjunction with *FEM_S* i.e. *FEM_S* + *FEM_V* combination. Therefore the two-element combination (*FEM_V* laid over *FEM_S*) is validated.

Cylindrical shell with clamped-free boundary conditions:

Properties: Total length (L) = 511.2 mm, thickness (t) = 1.5 mm, radius of curvature (R) = 216.2 mm, Young's modulus = 1.830E+11 N/m^2, Poisson's ratio = 0.28, density = 7492 kg/m^3

The cylindrical shell is of the type shown in Figure 2. In the validation test on the shell, some of the modes and corresponding frequencies (Hz) are obtained and compared with those in the relevant references available (see Table 1). The total thickness of the actual shell is distributed among the shell layers in the finite element model.

$^a m$	$n = 0$		
	Ref. [9]	Ref. [10]	Present
1	855.1	858.3	859.8
2	403.7	406.3	405.8
3	223.3	225.1	224.2
4	171.8	173.8	173.5
5	199.2	202.5	202.5
6	268.9	273.7	274.2

[a] *m,n are the circumferential and axial modes respectively*

Table 1: Modes of vibration and natural frequencies (Hz)

4. Numerical studies on partial coating of cylindrical shell

In the parametric studies presented, it is assumed that the weight of the damping treatment is a design constraint and is limited to about 1/4 the weight of the base shell. The case studies are separated according to the damping patch coverage area. In each case study, tests are conducted for different thicknesses (H_3) of the constraining layer. The thickness of the thin viscoelastic layer is kept fixed. In every test, the performance of the partial treatment for a specified set of target modes is investigated. The damping of the shell with partial coating is compared with that for full coverage (100%). Clamped-clamped boundary conditions for the shell are considered in this analysis. The modal parameter extraction procedures take into account the realistic cases of frequency and temperature dependence of the viscoelastic properties.

4.1. Clamped-clamped shell

The geometric details and some of the material properties of the complete shell (of the type shown in Figure 2) and the damping layer are given below.
Base shell structure:
Total length (L) = 2000 mm, thickness (t) = 1.75 mm, radius of curvature (R) = 250 mm, Young's modulus = 2.1E+11 N/m^2, Poisson's ratio = 0.3, density = 7850 kg/m^3
Constraining layer:
Young's modulus = 2.1E+11 N/m^2, Poisson's ratio = 0.3, density = 7850 kg/m^3
Viscoelastic layer:
Material- ISD-112, thickness of the viscoelastic layer = 0.3 mm.
The material properties of the viscoelastic layer are derived from the ISD-112 properties data sheet supplied by the 3M company. The temperature considered is 25° Celsius.

4.1.1. Vibration analysis of the undamped shell

The natural frequency values corresponding to the desired target modes are obtained and the results are shown in Table 2. The undamped shell is modelled using *FEM_S* elements.

Target mode count	Target modes		Frequency (Hz)
	Circumferential mode (m)	Axial mode (n)	
1	4	1	122.22
2	5	1	171.12
3	6	1	244.20
4	7	1	338.86
5	8	1	438.35

Table 2: Target modes and frequencies (Hz)

In order to realize the benefits of partial coating, efficient distribution of the damping treatment on the base shell is required. Therefore, in the present work the damping patches are distributed over regions of high strain energy intensity by referring to the *strain energy intensity distribution maps* derived for the purpose. A *strain energy intensity map* is obtained for each of the target modes, and these maps are then superimposed together to obtain an overall/combined strain energy distribution.

The strain energy over a discrete part of an undamped structure vibrating in its r th mode is yielded by the following quadratic form pertaining to any finite element:

$$SE^{(r)} = \{\psi\}_r^T [K_e]\{\psi\}_r \quad (1)$$

where r refers to the mode number, SE = strain energy, $\{\psi\}_r$ is the eigenvector of the finite element with the vector elements represented by all the values of nodal coordinates of the element. $\{\psi\}_r^T$ is the transpose of the eigenvector $\{\psi\}_r$. $[K_e]$ is the stiffness matrix of the element.

Equation (1) is used to obtain the combined strain energy distribution map for the five target modes of the clamped-clamped shell. The energy distribution is shown in Figure 3a / 3b for one of the octant portions of the complete shell (i.e. arc angle = 90° and length from the clamped end = $L/2$).

4.1.2. Damping analysis

Table 3 lists the case studies carried out for the damping analysis. The damping treatment is applied in the form of a band (circumferential strip) over the surface encompassing regions of high strain energy of the complete shell. Figure 3b indicates the layout of the damping band associated with the strain energy distribution of the representative portion of the complete shell.

Case study	Damping patch area coverage	Damping analysis tests for different thickness (mm) values of the constraining layer.		
		Test no. 1	Test no. 2	Test no. 3
1	100% (complete coating)	0.3	0.38	0.437 (max)
2	50%	0.55	0.77	0.875 (max)
3	58.33%	0.5	0.6	0.75 (max)
• max refers to the thickness limited by treatment weight constraint assumed for the case studies.				

Table 3: Configuration parameters used in damping analysis tests

In Case study 1 (full-coverage), the largest modal loss factors (η_{max}) were obtained for Test no. 3, i.e. for a constraining layer thickness of 0.437 mm. These modal damping results are compared with those from the test cases for partial coating. Figures 4 and 5 show plots of modal loss factors (η) vs. target modes for some of the test cases pertaining to Case studies 2 and 3 respectively, compared with η_{max} for full-coverage.

Figure 6 compares the test cases yielding maximum damping (η_{max}) in each case study.

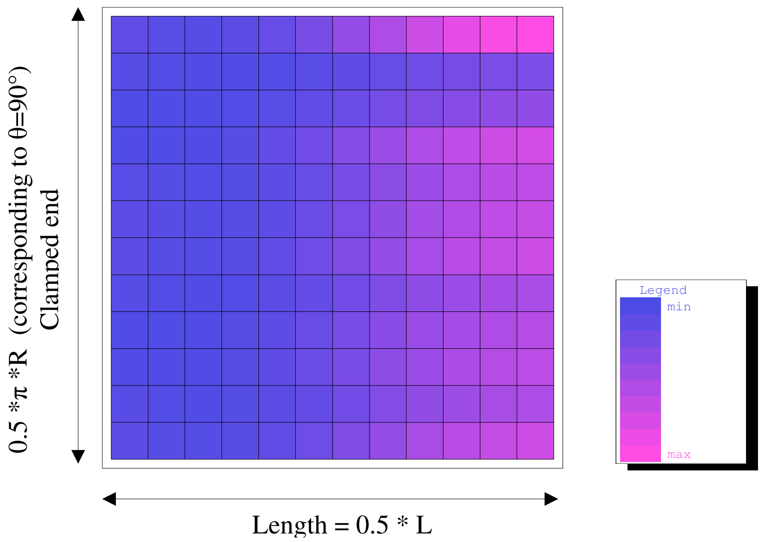

Figure 3a: Combined strain energy intensity distribution map for one of the octant portions of the complete shell.

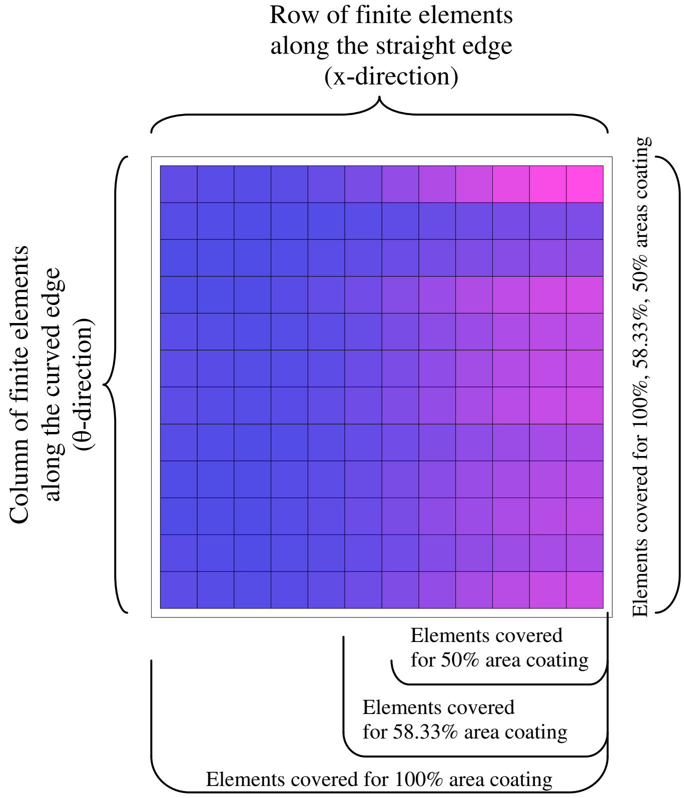

Figure 3b: Layout of damping layer band (element-wise) over the representative portion.

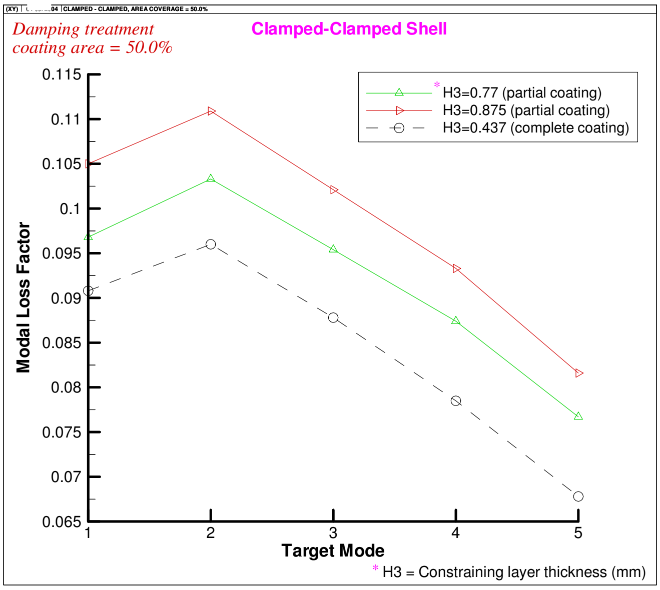

Figure 4: Modal loss factors for partial coating (treatment area: 50%) compared with maximum damping obtained for complete coating.

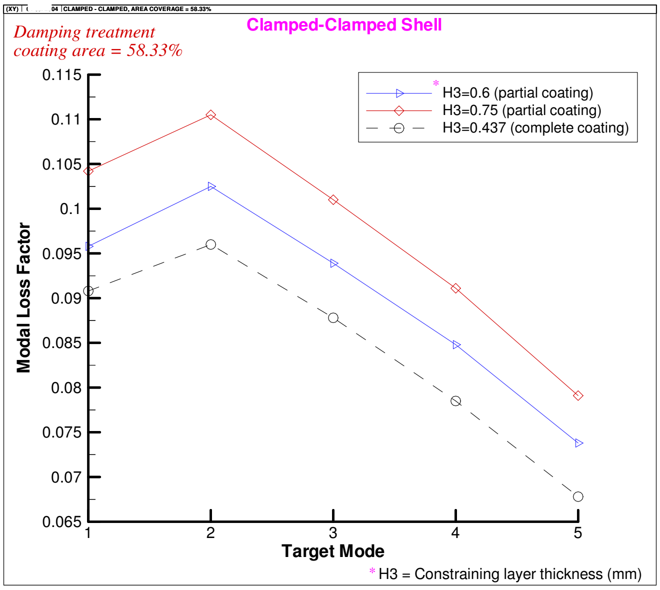

Figure 5: Modal loss factors for partial coating (treatment area: 58.33%) compared with maximum damping obtained for complete coating.

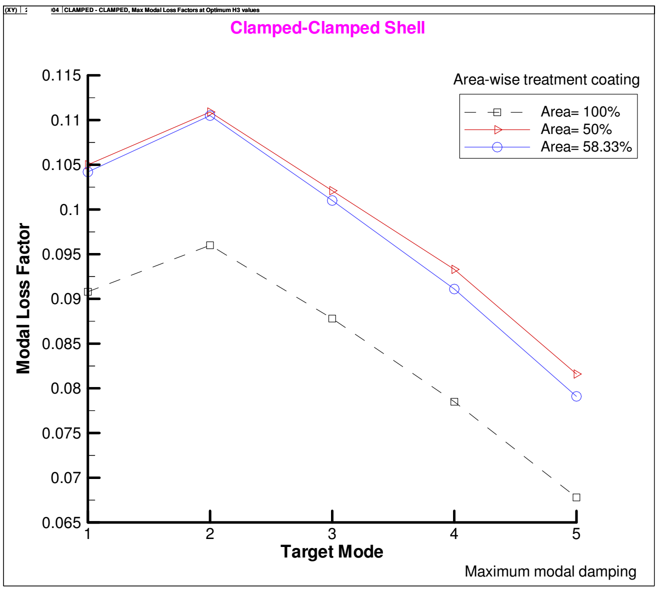

Figure 6: Comparison of maximum damping obtained for different areas of the damping patch distribution.

5. Conclusions

Modal loss factors obtained in the partial-coverage test cases (i.e. 50% coverage for constraining layer thickness H3 = 0.77 mm in Figure 4, and 58.33% coverage for H3 = 0.6 mm in Figure 5) are higher than the maximum modal damping obtained in the case of 100% coverage (at H3 = 0.437 mm). Therefore for a smaller coating area of the damping patch and less weight of the treatment, the modal damping for the target modes is higher than in the complete-coverage case. Also, Figure 6 shows that the modal damping for 50% coverage is higher than for 58.33%. This illustrates that an effective damping design that is constrained by treatment weight involves selecting a proper combination of area coverage, relative thickness and stiffness values of the layers of the damped configuration. A strain energy-based distribution of the damping treatment is shown to be beneficial.

Acknowledgements

The authors gratefully acknowledge the financial support given by the University of Hong Kong, including the provision of a Postgraduate Studentship.

References

[1] Š. Markuš, *Damping properties of layered cylindrical shells vibrating in axially symmetric mode*, Journal of Sound and Vibration. 48, No. 4, 1976, pp. 511-524.

[2] N. Alam, N.T. Asnani, *Vibration and damping analysis of a mutilayered cylindrical shell*, Parts I and II, AIAA Journal. 22, No. 6, 1984, pp. 803-810, pp. 975-981.

[3] T.C. Ramesh, N. Ganesan, *Vibration and damping analysis of cylindrical shells with a constrained damping layer*, Computers and Structures. 46, No. 4, 1993, pp. 751-758.

[4] J. Ro, A. Baz, *Optimum placement and control of active constrained layer damping using the modal strain energy approach,* Proceedings of SPIE. 332, 1998, pp. 9844-9855.

[5] A.B. Spalding, A.J. Mann III, *Placing small constrained layer damping patches on a plate to attain global or local velocity changes*, Journal of the Acoustical Society of America. 97, No. 6, 1995, pp. 3617-3624.

[6] F.K. Bogner, R.L. Fox, L.A. Schmit, *A cylindrical shell discrete element*, AIAA Journal. 5, No. 4, 1967, pp. 745-750.

[7] H. Kraus, *Thin elastic shells*, John Wiley and sons, Inc., 1967.

[8] K.R. Sivadas, N. Ganesan, *Dynamic analysis of circular cylindrical shells with material damping*, Journal of Sound and Vibration. 166, No. 1, 1993, pp. 103-116.

[9] H. Chung, *Free vibration analysis of circular cylindrical shells*, Journal of Sound and Vibration. 74, No. 3, 1981, pp. 331-350.

[10] T.C. Ramesh, N. Ganesan, *Finite element analysis of cylindrical shells with a constrained viscoelastic layer*, Journal of Sound and Vibration. 172, No. 3, 1994, pp. 359-370.